PAPER

Voltage-controlled current loops with nanofluidic diodes electrically coupled to solid state capacitors†

P. Ramirez,‡*[a] V. Gomez,‡[a] J. Cervera,‡[b] S. Nasir,‡[cd] M. Ali,‡[cd] W. Ensinger,‡[c] Z. Siwy‡[e] and S. Mafe‡*[b]

We describe experimentally and theoretically voltage–controlled current loops obtained with nanofluidic diodes immersed in aqueous salt solutions. The coupling of these soft matter diodes with conventional electronic elements such as capacitors permits simple equivalent circuits which show electrical properties reminiscent of a resistor with memory. Different conductance levels can be reproducibly achieved under a wide range of experimental conditions (input voltage amplitudes and frequencies, load capacitances, electrolyte concentrations, and single pore and multipore membranes) by electrically coupling two types of passive components: the nanopores (ionics) and the capacitors (electronics). Remarkably, these electrical characteristics do not result from slow ionic redistributions within the nanopores, which should be difficult to control and would give only small conductance changes, but arise from the robust collective response of equivalent circuits. Coupling nanoscale diodes with conventional electronic elements allows interconverting ionic and electronic currents, which should be useful for electrochemical signal processing and energy conversion based on charge transport.

Introduction

The use of nanodevices in chemical and biochemical applications is often difficult because of the response variability characteristic of nanostructures and the need to couple them with external equipment. These problems can be addressed by using simple equivalent circuits where more robust conventional components are efficiently coupled to the nanodevices. In this case, the resulting electrochemical characteristics are based not only on individual responses at the nanoscale, which are difficult to control in a reproducible way, but also on the robust collective response of the equivalent circuit.

We propose to study experimentally and theoretically the voltage-controlled current loops obtained by electrically coupling soft matter nanofluidic diodes with solid state capacitors. The design and characterisation of simple networks allow properties

[a]Departament de Física Aplicada, Universitat Politècnica de València, E-46022 València, Spain. E-mail: patraho@fis.upv.es

[b]Departament de Física de la Terra i Termodinàmica, Universitat de València, E-46100 Burjassot, Spain. E-mail: smafe@uv.es

[c]Department of Material- and Geo-Sciences, Materials Analysis, Technische Universität Darmstadt, D-64287 Darmstadt, Germany

[d]Materials Research Department, GSI Helmholtzzentrum für Schwerionenforschung, Planckstrasse 1, D-64291, Darmstadt, Germany

[e]Department of Physics and Astronomy, University of California, Irvine, CA 92697, USA

† Electronic supplementary information (ESI) available. See DOI: 10.1039/c6ra08277g

‡ The authors contributed equally to this work.

which are reminiscent of a resistor with memory using only two passive components, ionic diodes and external capacitors. The experimental characteristics obtained are robust and show that different ionic conductance levels can be achieved under a wide range of electrochemical conditions (input voltage amplitude and frequency, load capacitance, electrolyte concentration, and single pore and multipore membranes). The efficient coupling of the nanofluidic diodes with the external load capacitors facilitates the interconversion between ionic and electronic currents.

Hysteresis and memory effects are characteristic of the voltage-gated ion channels inserted in the bilayer lipid membrane of biological cells.[1,2] Because of the biomimetic nature of the nanofluidic diodes, the wide range of surface pore functionalisations currently available,[3–6] and the biocompatibility of aqueous ionic circuits with physiological salt solutions, the results should also be of interest for signal processing with electrically coupled biochemical and solid-state elements.[7–11] In particular, the external modulation of the nanofluidic rectification by chemical (electrolyte concentration and pH), thermal, optical, and electrical input signals[3–7,12–15] allows the conversion of input signals into electric responses which can be analysed using electronics components.[16–20]

Materials and methods

Nanopore fabrication

Stacks of six polyimide foils 12.5 μm thick (Kapton50 HN, DuPont) were irradiated under normal incidence with single

uranium ions of energy 11.4 MeV per nucleon at the linear accelerator UNILAC (GSI, Darmstadt). The range of the heavy ions in polyimide under these conditions was larger than the thickness of the foil stack and the energy loss of the ions was well above the threshold required for homogeneous track etching. A metal mask with a centered aperture of diameter 200 µm was placed in front of each stack for single-ion irradiation. The ion beam was blocked promptly as soon as a single ion passed through the foil stack and was registered by a particle detector behind the samples. This process produced tracks in multipore and single pore membranes which could be converted to approximately conical pores by asymmetric track-etching.[21,22] The pores radii estimated from the steady-state current (I)–potential (V) curves[22,23] were in the ranges 10–40 nm (tip) and 300–600 nm (base). The membrane area exposed to the solutions was 1 cm^2 approximately. The multipore membranes used here were obtained by irradiation with 10^4 heavy ions per cm^2, which after etching led to the pore density of 10^4 pores per cm^2. Fig. S1 in the ESI† shows an image of the multipore membrane surface. The etching process produced carboxylate residues on the pore wall surface which were ionised at pH = 7 (these residues were in neutral form at pH = 3, as confirmed by control I–V experiments where no electrical rectification was observed[19]). The solution pH was controlled by a Crison GLP22 pH-meter before and after each measurement.

Electrical measurements

The input voltages were applied by means of Ag|AgCl electrodes immersed in the bathing solutions at ambient temperature. Sinusoidal signals of frequencies in the range 3–60 mHz were considered. A picoammeter/voltage source (Keithley 6487/E) was used to record the I–V curves and a multimeter (Keithley 2000/E) was employed to measure the voltage across the capacitors. Because of the conical geometry, the electric potential is asymmetric along the pore axis (note that the surface charge density is constant but the pore radius changes along the axial direction of the cone). This asymmetry is responsible for the significant electrical rectification observed: the pore resistance was low when the current entered the cone tip while it was high when the current entered the cone base.[22,23] At low voltages, the cation flow constitutes the main contribution to current. At high enough voltages, however, the pores lose their selectivity for cations[22] and the current is carried by cations moving in the direction of the current and anions moving in opposite direction to the current. Fig. S2–S5 in the ESI† show the electrochemical characterization and stability of the multipore membranes used in the experiments. Fig. S2 and S3† show the steady-state I–V curves of the membranes 1 and 2 used in the half-wave multiplier of Fig. 1a in the case of a 0.1 M KCl (pH = 7) solution. Fig. S4† corresponds to the I–V curve of membrane 1 in 0.1 M KCl (pH = 7) and 0.1 M HCl solutions. Finally, Fig. S5† shows the reversal potential of membrane 1 for two multipore membrane positions and different KCl concentrations in the two chambers separated by the membrane.
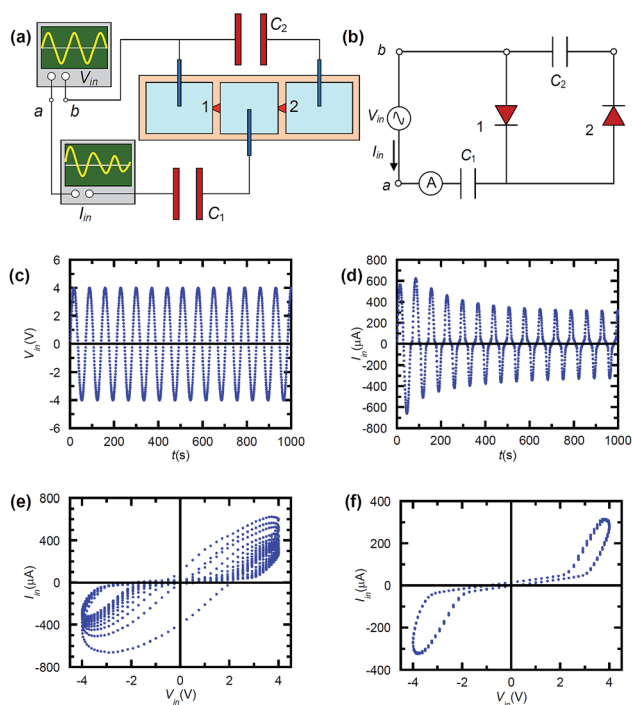

Fig. 1 Scheme of the experimental set-up showing the membrane diodes circuit acting as a half wave multiplier (a). The equivalent electrochemical circuit for the resulting voltage doubler (b). The time (t)-dependent applied voltage $V(t)$ (c) and the resulting current $I(t)$ (d). The input signal potential is a sinusoidal wave of frequency $\nu_0 = 14$ mHz. The typical transient behaviour for the resulting voltage-controlled current loops (e). The steady-state voltage-controlled current loops (f). The experiments correspond to a KCl electrolyte solution of concentration $c_0 = 0.1$ M at pH = 7. The capacitances of the capacitors used are $C_1 = C_2 = 5$ mF.

Results and discussion

Fig. 1a shows a scheme of the experimental set-up. Only one nanofluidic diode is shown in the multipore membranes 1 and 2 for the sake of clarity. The equivalent electrical circuit with the load capacitors acts as a half wave multiplier (voltage doubler) when the output voltage is measured between the terminals of capacitor C_2 (Fig. 1b, see ref. 24 for more details). Fig. 1c shows the applied voltage $V(t)$ and Fig. 1d the measured current $I(t)$ as functions of the time t. The results are obtained for a KCl electrolyte solution of concentration $c_0 = 0.1$ M at pH = 7. The capacitances of the capacitors used are $C_1 = C_2 = 5$ mF. The typical transient (Fig. 1e) and steady-state (Fig. 1f) curves showing voltage-controlled current loops are reminiscent of a resistor with memory[25] and have been obtained here using only two types of passive components.

The reproducibility of the measurements was checked by measuring the experimental curves several times (see ESI† for specific examples). The transient voltage-controlled current loops of Fig. 1e depend on the initial conditions (particularly on the initial charge of the capacitors) but the steady-state voltage-controlled current loops of Fig. 1f were found to be similar in all experiments performed under a given set of experimental conditions.

Note that the two nanofluidic diodes in Fig. 1b are connected with opposite polarities, which gives a negligible rectification of the total electric current in Fig. 1f. The polarities of the diode membranes change with time and this fact introduces different characteristic times for the capacitors charging and discharging, leading to the observed voltage-controlled loops. If the two diode membranes are oppositely biased, the resulting current is small (see the central region of the curve in Fig. 1f). The current becomes large only in the loop regions where one of the two capacitors is discharged following the easy-current direction of the corresponding diode membrane.

Memory effects due to history-dependent ion transport have been observed previously in the I–V curves of conical nano-pores.[25] In particular, a cross-point potential separating current loops with low and high conductivity states was explained in terms of the finite mobility of ions within the charged nanopore under different potentials and electrolyte concentrations.[25] However, the results presented here have three important differences with respect to those of ref. 25 for a single pore (see also ref. 26): (i) Fig. 1e and f show non-crossing pinched curves; (ii) the current loops appear only at the ends of a central plateau region characterised by small currents; and (iii) the different conductance states in Fig. 1e and f do not result from slow ion redistribution processes within an individual nanopore, which might be difficult to control in a reproducible way and would give only relatively small conductance changes.[25] On the contrary, the plateaus and conductance transitions obtained here are robust collective characteristics of a simple circuit where the pores acting as nanofluidic diodes are coupled with the load capacitors. In this sense, it is not possible to quantitatively compare the significant conductance changes obtained here with those of ref. 25 because of their different origin.

Remarkably, the conductance transitions occur at a well-defined threshold potential and show off/on resistance ratios $R_{\text{off}}/R_{\text{on}}$ close to 100, which is much higher than the typical rectification ratio obtained with nanofluidic membranes only.[18,22] In this way, the reliability and the operational properties of the membrane diodes can be improved significantly by the coupling between the ionics and electronics elements in Fig. 1a.

The stability of the multipore membranes and the reproducibility of the voltage-controlled current loops in Fig. 1e and f were checked further by conducting the experiments several times (see Fig. S6–S8 in the ESI†). The experimental data obtained within a two month period using different cells and electrodes showed a good reproducibility (see Fig. S9†). It is important to note that there are other independent factors, which influence the current rectification in conical nanopores and may affect the observed voltage-controlled current loops. We consider here the voltage amplitude, salt concentration, capacitor characteristics, and signal frequency. Additionally, the pH of the solution may also influence pore selectivity and rectification (see Fig. S5†).

The emerging electrical characteristics can be modulated externally in a reproducible way by using different voltage amplitudes and electrolyte concentrations. The experimental (Fig. 2a) and theoretical (Fig. 2b) curves show the effects of the applied voltage amplitude on the current loops while the effects of electrolyte concentration are shown in Fig. 2c.
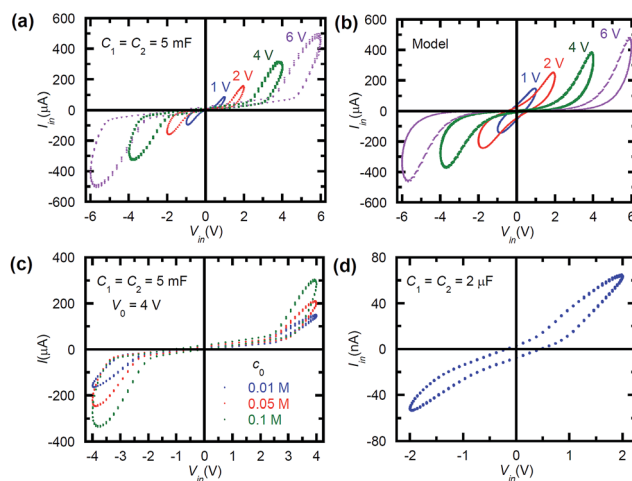

Fig. 2 Experimental and theoretical results for the electrochemical circuit of Fig. 1 (see the ESI† for the model equations of the equivalent electric circuits). The effect of the voltage amplitude on the current loops (a). The theoretical current loops curves (b). The effect of the electrolyte concentration on the current loops for the input voltage amplitude $V_0 = 4$ V (c). The experimental results for the case of single nanofluidic diode membranes (d). Note the change in the order of magnitude of the capacitances due to the different scaling in the number of pores.

As expected, increasing the concentration c_0 produces an increase in the absolute values of the current because of the increase in the number of ionic carriers available and a decrease in the extension of the low conductance region because of the decrease in the pore rectification (Fig. 2c). Fig. 2d shows the significant scaling effect obtained for a membrane with only a single nanofluidic diode. Note the different scales of the currents and capacitances in Fig. 2d with respect of those in Fig. 2a. The distinct scales obtained are in agreement with the increase in the number of effective pores available for ion transport in the multipore membrane, which should be close to 10^4 for the total exposed area.

To check further the efficient coupling between the different circuit components under different electrical arrangements, Fig. 3a corresponds to an alternative experimental set-up where the membranes with nanofluidic diodes are coupled with the load capacitors to give an equivalent circuit showing full wave multiplier characteristics when the output voltage is measured
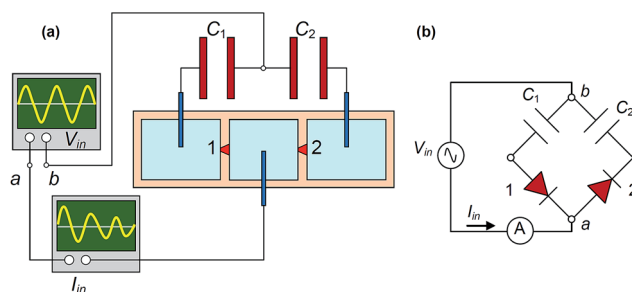

Fig. 3 Scheme of the experimental set-up showing the membrane diodes circuit acting as a full wave multiplier (a) and the equivalent electrochemical circuit (b).

between the terminals of capacitors C_1 and C_2 (Fig. 3b, see ref. 24 for more details).

The experimental current loops are obtained parametrically in the input voltage amplitude and correspond to the cases of balanced (Fig. 4a–c) and unbalanced (Fig. 4d) capacitances.

The reliability of the experimental approach followed here is demonstrated using the circuit sketched in a half wave quadrupler circuit (Fig. 5a and b)[24] with four multipore membranes producing the steady-state current loops of Fig. 5c. In this case, the different impedance of the capacitors used in the arrangement gives currents higher than those of the half wave voltage doubler in Fig. 2a.

Finally, Fig. 6a and b show the experimental and theoretical results obtained for the circuit of Fig. 1a at three different frequencies. Note that the equivalent impedance due to the capacitors in the circuit should be inversely proportional to the product of the frequency and the capacitance: the shrinking in the current loops observed at high frequencies in Fig. 6a is consistent with the behaviour observed at high capacitance in

Fig. 6 Experimental (a) and theoretical (b) results obtained for the circuit of Fig. 1a at three different frequencies. Experimental results obtained with a KCl electrolyte solution of concentration $c_0 = 0.1$ M at pH = 7 and the input voltage amplitude $V_0 = 2$ V.

Fig. 4a–c. The loops gradually disappear with the increase in the signal frequency but significant membrane rectification is still observed, suggesting that the equivalent circuit characteristics are robust and can be achieved by using different electrical schemes and time scales.

Conclusions

It is of current interest to design and characterise hybrid circuits where micro and nanofluidic pores coupled with conventional electronic elements perform electrochemical signal processing and charge-based energy conversion tasks.[8,9,17–19,24] We have described experimentally and theoretically the voltage-controlled current loops obtained with soft matter nano-diodes immersed in aqueous salt solutions at ambient temperature. The coupling of these liquid state elements with solid state capacitors gives different ionic conductance levels under a range of input voltage amplitudes and frequencies, capacitances, and electrolyte concentrations in the case of single pore and multipore membranes.

Remarkably, the current loops do not result from ionic redistribution processes within the nanopore, which should be slow and difficult to control in practice, giving only small, non-reproducible conductance changes. On the contrary, these conductance states are emerging collective characteristics of a simple circuit with only two types of elements: the nanopores acting as nanofluidic diodes and the load capacitors. The efficient coupling between the ionics (nanopores) and the electronics (capacitors) in simple electrochemical circuits allows properties reminiscent of a resistor with memory which shows high off/on switching resistance ratios by using only two passive components. This coupling should facilitate interconverting ionic and electronic currents in signal processing and charge-based energy conversion procedures based on the external modulation of the nanofluidic resistances.[3,13–15,19,27]
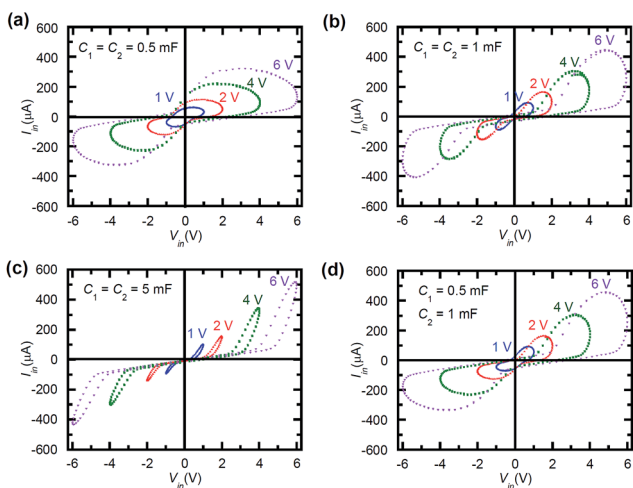

Fig. 4 Experimental results for the electrochemical circuit of Fig. 3. The current loop curves are parametric in the voltage amplitude. The cases of balanced (a–c) and unbalanced (d) capacitances are shown.
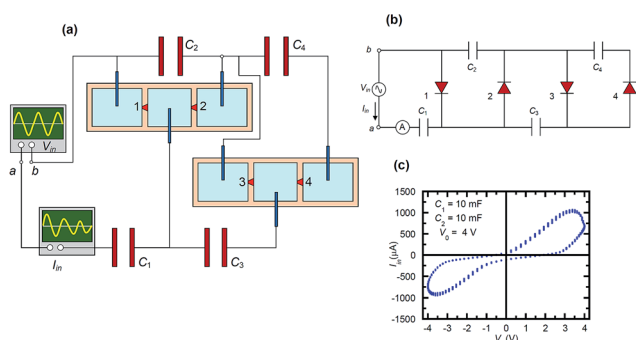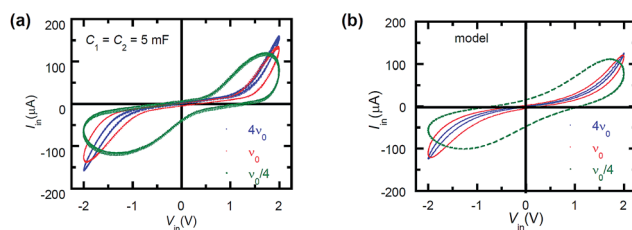

Fig. 5 Scheme of the experimental set-up showing the electrochemical circuit acting as a half wave quadrupler (a) and the equivalent electrical circuit (b). Experimental results obtained with a KCl electrolyte solution of concentration $c_0 = 0.1$ M at pH = 7 and the input voltage amplitude $V_0 = 4$ V (c).

Acknowledgements

Notes and references

1 D. Fologea, E. Krueger, Y. I. Mazur, C. Stith, Y. Okuyama, R. Henry and G. J. Salamo, *Biochim. Biophys. Acta, Biomembr.*, 2011, **1808**, 2933.

2 M. A. Pustovoit, A. M. Berezhkovskii and S. M. Bezrukov, *J. Chem. Phys.*, 2006, **125**, 194907.

3 P. Ramirez, J. Cervera, M. Ali, W. Ensinger and S. Mafe, *ChemElectroChem*, 2014, **1**, 698.

4 C. R. Martin and Z. S. Siwy, *Science*, 2007, **317**, 331.

5 X. Hou and L. Jiang, *ACS Nano*, 2009, **3**, 3339.

6 H. Zhang, Y. Tian and L. Jiang, *Nano Today*, 2016, **11**(1), 61–81.

7 H. Chun and T. D. Chung, *Annu. Rev. Anal. Chem.*, 2015, **8**, 441.

8 M. Tagliazucchi and I. Szleifer, *Mater. Today*, 2015, **18**, 131.

9 N. Misra, J. A. Martinez, S.-C. J. Huang, Y. Wang, P. Stroeve, C. P. Grigoropoulos and A. Noy, *Proc. Natl. Acad. Sci. U. S. A.*, 2009, **106**, 13780.

10 S. Senapati, S. Basuray, Z. Slouka, L.-J. Cheng and H.-C. Chang, *Top. Curr. Chem.*, 2011, **304**, 153.

11 D. G. Haywood, A. Saha-Shah, L. A. Baker and S. C. Jacobson, *Anal. Chem.*, 2015, **87**, 172.

12 G. Pérez-Mitta, J. S. Tuninetti, W. Knoll, C. Trautmann, M. E. Toimil-Molares and O. Azzaroni, *J. Am. Chem. Soc.*, 2015, **137**, 6011.

13 M. Ali, S. Nasir, P. Ramirez, I. Ahmed, Q. H. Nguyen, L. Fruk, S. Mafe and W. Ensinger, *Adv. Funct. Mater.*, 2012, **22**, 390.

14 M. Ali, S. Nasir, P. Ramirez, J. Cervera, S. Mafe and W. Ensinger, *J. Phys. Chem. C*, 2013, **117**, 18234.

15 M. Ali, I. Ahmed, S. Nasir, P. Ramirez, C. M. Niemeyer, S. Mafe and W. Ensinger, *ACS Appl. Mater. Interfaces*, 2015, **7**, 19541.

16 T. Albrecht, *ACS Nano*, 2011, **5**, 6714.

17 S. G. Lemay, *ACS Nano*, 2009, **3**, 775.

18 V. Gomez, P. Ramirez, J. Cervera, S. Nasir, M. Ali, W. Ensinger and S. Mafe, *Sci. Rep.*, 2015, **5**, 9501.

19 V. Gomez, P. Ramirez, J. Cervera, S. Nasir, M. Ali, W. Ensinger and S. Mafe, *Nano Energy*, 2015, **16**, 375.

20 K. Tybrandt, R. Forchheimer and M. Berggren, *Nat. Commun.*, 2012, **3**, 871.

21 P. Apel, *Radiat. Meas.*, 2001, **34**, 559.

22 J. Cervera, B. Schiedt, R. Neumann, S. Mafe and P. Ramirez, *J. Chem. Phys.*, 2006, **124**, 104706.

23 M. Ali, P. Ramirez, S. Mafe, R. Neumann and W. Ensinger, *ACS Nano*, 2009, **3**, 603.

24 P. Ramirez, V. Gomez, C. Verdia-Baguena, S. Nasir, M. Ali, W. Ensinger and S. Mafe, *Phys. Chem. Chem. Phys.*, 2016, **18**, 3995.

25 D. Wang, M. Kvetny, J. Liu, W. Brown, Y. Li and G. Wang, *J. Am. Chem. Soc.*, 2012, **134**, 3651.

26 D. Momotenko and H. H. Girault, *J. Am. Chem. Soc.*, 2011, **133**, 14496.

27 A. Zhang and C. M. Lieber, *Chem. Rev.*, 2016, **116**, 215.